energies

MDPI

Article

Parameters Identification of Proton Exchange Membrane Fuel Cell Model Based on the Lightning Search Algorithm

Banaja Mohanty [1], Rajvikram Madurai Elavarasan [2,*], Hany M. Hasanien [3,*], Elangovan Devaraj [4], Rania A. Turky [5] and Rishi Pugazhendhi [6]

[1] Department of Electrical Engineering, Veer Surendra Sai University of Technology (VSSUT), Burla 768018, India
[2] School of Information Technology and Electrical Engineering, The University of Queensland, St Lucia, QLD 4072, Australia
[3] Electrical Power and Machines Department, Faculty of Engineering, Ain Shams University, Cairo 11517, Egypt
[4] TIFAC CORE and School of Electrical Engineering, Vellore Institute of Technology (VIT), Vellore 632014, India
[5] Electrical Engineering Department, Faculty of Engineering and Technology, Future University in Egypt, Cairo 11835, Egypt
[6] Research & Development Division (Power & Energy), Nestlives Private Limited, Chennai 600091, India
* Correspondence: rajvikram787@gmail.com or r.maduraielavarasan@uqconnect.edu.au (R.M.E.); hanyhasanien@ieee.org (H.M.H.)

Abstract: The fuel cell is vital in electrical distribution networks as a distributed generation in today's world. A precise model of a fuel cell is extensively required as it rigorously affects the simulation studies' transient and dynamic analyses of the fuel cell. This appears in several microgrids and smart grid systems. This paper introduces a novel attempt to optimally determine all unknown factors of the polymer exchange membrane (PEM) fuel cell model using a meta-heuristic algorithm termed the Lightning search algorithm (LSA). In this model, the current–voltage relationship is heavily nonlinear, including several unknown factors because of the shortage of fuel cell data from the manufacturer's side. This issue can be treated as an optimization problem, and LSA is applied to detect its ability to solve this problem accurately. The objective function is the sum of the squared error between the estimated output voltage and the measured output voltage of the fuel cell. The constraints of the optimization problem involve the factors range (lower and upper limit). The LSA is utilized in minimizing the objective function. The effectiveness of the LSA-PEM fuel cell model is extensively verified using the simulation results performed under different operating conditions. The simulation results of the proposed model are compared with the measured results of three commercial fuel cells, such as Ballard Mark V 5 kW, BCS 500 W and Nedstack PS6 6 kW, to obtain a realistic study. The results of the proposed algorithm are also compared with different optimized models to validate the model and, further, to determine where LSA stands in terms of precision. In this regard, the proposed model can yield a lower SSE by more than 5% in some cases and high performance of the LSA-PEMFC model. With the results obtained, it can be concluded that LSA prevails as a potential optimization algorithm to develop a precise PEM fuel cell model.

Keywords: parameters identification; lightning search algorithm (LSA); PEM fuel cell; optimization algorithm; fuel cell model

Citation: Mohanty, B.; Madurai Elavarasan, R.; Hasanien, H.M.; Devaraj, E.; Turky, R.A.; Pugazhendhi, R. Parameters Identification of Proton Exchange Membrane Fuel Cell Model Based on the Lightning Search Algorithm. *Energies* **2022**, *15*, 7893. https://doi.org/10.3390/en15217893

Academic Editor: Attilio Converti

Received: 9 October 2022
Accepted: 23 October 2022
Published: 24 October 2022

1. Introduction

In the wake of the climate crisis, shifting the energy generation scenario of conventional energy resources to clean energy resources is one of the most promising approaches to sustaining humanity [1,2]. Solar and wind energy harvesting technologies have been well-developed among clean energy resources. On the other hand, abundant and environmentally friendly hydrogen fuel prevails as clean energy and a sustainable energy

resource [3]. However, the scale of hydrogen energy utilization is extremely small compared with other renewable energy sources and also lags in commercialization. However, the cost of storing the hydrogen gas and maintaining safety precautions is still a significant barrier. When humanity can harness hazardous and sophisticated nuclear energy with enormous precision in operation, hydrogen energy can also be driven by a much safer and more affordable nature that requires only a fraction of innovations. One underpinning technology that utilizes hydrogen energy to generate electricity through electrochemical reactions is Fuel Cells (FCs). It is a noble technology as the output is electric power and water in most cases (depending on the fuel cells and the fuel used). The direction of developments occurring in the FC domain favors the transportation sector, but another critical application of fuel cells involves distributive generation (DG), which needs more attention.

The Proton Exchange Membrane FC (PEMFC) and Alkaline FC (AFC) are common types of fuel cells that use hydrogen as fuel. Because of its quick start-up, low operating temperature, and high efficiency, PEMFC prevails as a highly preferable fuel cell [4]. As the fuel cell experience a decreasing output voltage with increasing current load, also known as the fuel cell's polarization characteristics, they request power conditioning control units for DG applications [5]. The V-I characteristics of a fuel cell should be well-established in all scenarios to effectively function and design power conditioning units. In this case, several unknown parameters are needed to be determined for calculating the polarization characteristics, but this always prevails as a puzzle for the research community to extract these parameters accurately with minimal effort. The prime reason for this issue is tricky to solve due to the high non-linearity and non-convexity nature of the unknown parameters in context with the complex conversion behavior of fuel cells. In brief, these unknown parameters establish the relationship between V-I characteristics, fuel input conditions, and healthy operation of fuel cells whose data with various influencing factors are not envisioned by the manufacturers. All of these necessitate a reliable mathematical model to extract the parameters through various analytical methods.

Over time, numerous models were developed and analyzed by the researchers. Springer et al. developed a one-dimensional steady-state model of PEMFC based on isothermal parameterization [6]. Panagiotis et al. performed parametric analysis on two dynamic fuel cell models in which one is based on electrical equivalent and the other uses a semi-empirical approach [7]. A real-time model is designed and validated using various techniques by Kumar et al. [8]. Meanwhile, a study shifted the attention to improving the fuel cells' stability and performance by enhancing the humidification of the polymer electrolyte membrane of PEMFCs [9]. In this study, multiple input/output nonlinear fourth-order models are designed based on air circulation mass and heat dynamics, and a nonlinear control strategy is employed to obtain an experimentally verified low-temperature PEMFC model.

All the approaches presented in the above-stated models and other validated models involve concepts ranging from thermodynamics, mass and heat transfer, and momentum conservation to the precise simulation model. Such an approach introduces extreme complexity and requires substantial computational power, gradient information, and the need for initial conditions. On the other hand, all uncertain processes cannot be modeled by using analysis to back up these concepts. This further introduces increased constraints and assumptions which affect the model's practicality, and the gap is further expanded between the real-time scenario and theoretical environment. However, irrespective of the various model approaches, the objective will be to develop as precise a model as possible to identify the unknown parameters.

To reduce the computational power, avoid local trapping, and obtain accurate results, optimization algorithms would help the models to converge the analysis much faster by eliminating specific defined pathways or rules governed by the algorithms. In context with it, the researchers developed several parameter identification strategies. For instance, parameter extraction through decomposition technique and nature-inspired optimization method for electrochemical model [10], parameter identification through shuffled

multi-simplexes search algorithm [11], fuel cell inconsistency analysis [12], and AI-based optimization modeling to obtain maximum power density [13] are presented. As computers are getting smarter with intelligence, meta-heuristic algorithms are born with profound applications associated with optimizing high non-linearity problems. Meta-heuristic algorithms do not require any gradient information, no requirements of information related to a specific search domain, or convexity/continuity of objective functions [14].

Further, meta-heuristic algorithms are robust, easy to implement, and more efficient and effective in solving unknown parameter problems. Moreover, a study surveyed the parameter identification techniques using various algorithms and their perspectives concerning solid oxide fuel cells [15]. Regarding PEMFC, fewer studies have analyzed the feasibility of these algorithms to develop precise models and extract unknown parameters. Table 1 represents the various meta-heuristic algorithms with their inspiration, typical approach, features, limitations, and implications in fuel cells.

Besides the discussed algorithms, hybrid algorithms such as the hybrid Teaching Learning-Differential Evolution optimization algorithm also exist [16–18]. Another improved optimization algorithm implemented by researchers in the domain of fuel cells involves a fluid search optimization algorithm [19], seagull optimization algorithm [20], Krill herd optimization algorithm [21], deer hunting optimization algorithm [22], global extremum-seeking algorithm [23], Cuckoo search algorithm [24] and Nelder-Mead algorithm [25]. Hence, there exists a research gap to identify the best-suited algorithm, particularly for PEMFC, and to identify other algorithms in existence that are not employed in the fuel cell domain and how they are effective in identifying the parameters of PEMFC when compared with other algorithms. The development of meta-heuristic algorithms is highly welcomed if they yield better results.

Table 1. Various meta-heuristic algorithms and their inspiration, approaches, features, limitations and implications in fuel cells.

Optimization Algorithm	Inspiration (If Any)	Approach in the Algorithm	Features	Limitations	Algorithm Implementation in Fuel Cell Application	References
Genetic algorithm	Inspired from evolution	Selection, crossover, and mutation are the important steps	It outpaces the radial basis function neural network approach. It is efficient, possesses a simple structure, high accuracy, validity, and stability	Lacks high robustness	Static and dynamic modeling of SOFC	[26–28]
Differential evolution algorithm	Inspired from evolution	Initialization, mutation, crossover, and selection	Higher convergence speed, accuracy, fast parameter turning, and robustness	Not specified	Modeling performance metrics of PEMFC and parameter extraction in various fuel cells	[29,30]
Particle swarm optimization algorithm	Inspired by swarm intelligence	Based on particle position and velocity and updating the parameters for the best position	Many learning strategies are implemented to improve the algorithm's effectiveness. A proper balance between global exploration and local exploitation is observed.	Low convergence speed and low searching efficiency comparatively	Parameter identification for SOFC and PEMFC	[31–33]
Artificial bee colony algorithm	Inspired by the foraging behavior of bees	Exploration and exploitation is accompanied by employed bees, onlooker bees, and scout bees. Various bees update their position following different paths.	Simple, very good at global exploration and faster convergence rate.	Sometimes converges prematurely and causes weak local exploration ability	The hybrid algorithm employed to identify the parameters for PEMFC	[34,35]
Grasshopper optimization algorithm	Inspired by the foraging behavior of grasshoppers	Based on attractive and repulsive interaction. The search agents move rapidly during Exploration and tend to move locally during exploitation	Simplicity with minimum parameters and maximum classification performance	Lacks high accuracy	Parameter identification for SOFC	[36–38]
Chaotic binary shark smell optimization algorithm	Inspired by prey hunting strategy of sharks	Initialization, shark movement in terms of forwarding and rotational towards the odor concentrator	High efficiency, simple structure, and high stability	Assumptions reduce the robustness of the algorithm	Parameter identification for PEMFC and SOFC	[38,39]
Interior search algorithm	Inspired by interior space decoration strategy by architectures	Defining bounds, identifying the fittest element, composition, and mirror group work to find the better view	High accuracy and convergence speed, the minimal tuning parameter	Sometimes converges prematurely	Parameter extraction for fuel cells	[40,41]
Salp swarm algorithm	Inspired by the foraging behavior of forming collaborative chains by a group of salps	The chain consists of two elements, namely, leaders and followers.	Easy to tune the parameter and faster convergence speed	Accuracy is the limitation	Parameter extraction for fuel cells	[41,42]
Grey wolf optimization algorithm	Inspired by the collective hunting strategy of grey wolves	Prey identification, tracking and chasing, encircling and attacking the prey	Simple structure, good global exploration, high flexibility	Moderate accuracy and the speed of convergence will slow down eventually	Parameter extraction for fuel cells	[41,43]

Table 1. *Cont.*

Optimization Algorithm	Inspiration (If Any)	Approach in the Algorithm	Features	Limitations	Algorithm Implementation in Fuel Cell Application	References
Multiverse optimization algorithm	Inspired by multiverse theory in cosmology	A black hole and white hole represent global exploration, while the wormhole represents local exploitation. The inflation rate helps in determining the ranking.	Less computation, minimum parameters to tune, and simplistic construction	Convergence speed is comparatively slow	Identifying optimal parameters for the PEMFC model	[44]
Competitive swarm optimizer algorithm	It is a simplified version of the Particle swarm optimization algorithm	A pairwise competition mechanism is established to simplify the algorithm structure and consistency	High accuracy, robustness, and convergence speed	Not favorable for complex multi-nodal optimization and would result in low search efficiency	Parameter identification for SOFC	[45,46]
Whale optimization algorithm	Inspired by the bubble-net hunting strategy of humpback whales	Encircling the prey, creating a bubble net creation, capturing the victim	High computation accuracy and convergence speed	Global exploration is not much effective comparatively	Semi-empirical PEMFC model for unknown parameter identification	[47,48]
Biogeography based optimization	Inspired by Island biogeography	Based on two operators, namely, migration and mutation, and accommodated with immigration and emigration rate	The solution is moderately accurate	Less convergence speed and lacks local exploitation	Model parameter estimation for fuel cells	[49,50]
Satin bowerbird optimizer	Inspired by the mechanism of bird mating	Other bowers prefer Bowers with higher fitness.	Simple to tune the parameters, robust and random nature of the algorithm, can effectively engage with multi-modal optimizations	Complex parameter setting	SOFC parameter extraction for steady-state and dynamic models	[51,52]
Backtracking search algorithm	-	It uses present and historical population data to perform iteration and to achieve diversity also with the incorporation of random mutation	Good balance between exploitation and Exploration, reliable and high accuracy	Convergence speed is comparatively slow	Parameter estimation for PEMFC	[53]
Teaching learning-based optimization	Inspired by a teaching-learning process in the classroom	Two involved processes, namely teaching and learning. Sometimes ranking mechanism is also introduced	Simple construction, high accuracy, robustness, and better convergence speed. Many hybrid features are proposed in context with the Teaching-learning process	It might easily get trapped at the local optimum	Parameter identification of SOFC	[54,55]

The objective of this study is to obtain a precise model and validate it with an experimental comparison with the support of a novel lightning search algorithm (LSA). This proposed algorithm is motivated by the concept of lightning stroke phenomena [56]. This algorithm efficiently solved many optimization problems. Many comparisons have been made between the proposed algorithm and other optimization algorithms, expressing its superiority [56,57]. The LSA possesses many advantages its lower consuming time, lower number of fine-tuned parameters, and simple procedure. Moreover, it has been applied to solve many power systems optimization problems, such as its application to the nuclear power system [58], speed control of induction motor drives [59], optimal placement of electric vehicle charging stations [60], the optimal location of DG in distribution systems [61], and optimization of wind farm layout [62]. This algorithm has not been utilized in the expertise of fuel cells (as of the authors' knowledge), and the research community needs precise and reliable output through various algorithms. So, this study contributes to the fuel cell domain to identify the algorithm's effectiveness in extracting the unknown parameters of the fuel cells and verifies whether this algorithm satisfies the practical scenarios and whether it is relatively reliable with other algorithms. The contributions of this study can be claimed as follows:

- Implementation of lightning search algorithm (LSA) for PEM fuel cell application;
- Developing a precise model and extracting the unknown parameters resulted from the shortage of manufacturer's data;
- Comparison of the results obtained from LSA and other algorithms to project a better picture for the researchers about where its precision stands.

The paper is established as follows: Section 2 presents the PEMFC model in the steady state condition. In Section 3, the problem formulation and the proposed LSA are described. Section 4 depicts the simulation results of the proposed LSA-PEMFC model and its comparison with the experimental results for different commercial PEMFCs. Finally, a conclusion of the research work is introduced in Section 5.

2. PEMFC Model

The mathematical model of the PEMFC is developed to express the main steady-state characteristics of the PEMFC [63]. The proposed model includes the voltage drop of the FC named: (1) activation overpotential (v_{act}), (2) ohmic voltage (v_{Ω}), and (3) concentration overpotential (v_{con}).

The mathematical equation of the PEMFC stack voltage can be written as follows:

$$V_{Stack} = N_{cells}.(E_{Nernst} - v_{act} - v_{\Omega} - v_{con}) \quad (1)$$

where N_{cells} represents the total number of series-connected cells and E_{Nernst} devotes the reversible voltage, which is calculated by using the equation as follows:

$$E_{Nernst} = 1.229 - 0.85 \times 10^{-3}\left(T_{fc} - 298.15\right) + 4.3085 \times 10^{-5} T_{fc} ln\left(P_{H_2}\sqrt{P_{O_2}}\right) \quad (2)$$

The voltage drop of the PEMFC can be calculated as follows [64]:

$$v_{act} = -\left[\xi_1 + \xi_2 T_{fc} + \xi_3 T_{fc} ln(C_{O_2}) + \xi_4 T_{fc} ln\left(I_{fc}\right)\right] \quad (3)$$

where $C_{O_2} = \frac{P_{O_2}}{5.08 \cdot 10^6} \cdot \exp\left(498/T_{fc}\right)$

$$v_{\Omega} = I_{fc}(R_m + R_c);\ R_m = \frac{\rho_m l}{M_A} \quad (4)$$

where $\rho_m = \frac{181.6\left[1+0.03\left(\frac{I_{fc}}{M_A}\right)+0.062\left(\frac{T_{fc}}{303}\right)^2\left(\frac{I_{fc}}{M_A}\right)^{2.5}\right]}{\left[\lambda-0.634-3\left(\frac{I_{fc}}{M_A}\right)\right]e^{4.18\cdot\frac{T_{fc}-303}{T_{fc}}}}$.

$$v_{con} = -\beta \cdot ln\left(1 - \frac{J}{J_{max}}\right) \tag{5}$$

where T_{fc} represents the FC temperature (K), P_{H_2} and P_{O_2} point out partial pressures of both hydrogen and oxygen (atm), I_{fc} represents the current of the FC (A), M_A describes the membrane area (cm^2), C_{O_2} is oxygen concentration (mol/cm^3), ξ_{1-4} are numerical coefficients, R_m represents the resistance of the membrane (Ω), R_c is resistance due to connections (Ω), l representthe thickness of the membrane (cm), ρ_m describes its resistivity $(\Omega \cdot cm)$, λ is a coefficient that concerns water content and humidity, β represents a constant coefficient, and J and J_{max} represents the real and maximum value of the current density (A/cm^2).

In this proposed PEMFC model, seven parameters define the polarization characteristics of the PEMFC. These parameters are ξ_1, ξ_2, ξ_3, ξ_4, λ, R_c and β. These parameters affect the model's accuracy and efficiency. Therefore, their values should be identified in a very accurate way to obtain a precise model of the PEMFC.

3. Problem Formulation and the LSA

3.1. Problem Formulation

The principal objective function of the optimization problem under study is based on the sum of square error (SSE) between the measured output FC voltage and its estimated output voltage. The design variables of the optimization problem consist of ξ_1, ξ_2, ξ_3, ξ_4, λ, R_c and β The proposed LSA minimizes this objective function under the design variables constraints. These constraints include the upper and lower limit of each design variable. The following formula mathematically formulates the objective function:

$$SSE = \left(\sum_{i=1}^{N_{samples}} [V_{FC,meas}(i) - V_{FC,est}(i)]^2\right) \tag{6}$$

where $N_{samples}$ represents the total number of measured data, i is an iteration index, $V_{FC,meas}$ represents the measured output voltage of the PEMFC, and $V_{FC,est}$ depicts the estimated output voltage of the proposed LSA-PEMFC model.

3.2. The Lightning Search Algorithm (LSA)

The LSA is a meta-heuristic algorithm that has a natural phenomenon. The LSA is based on the mechanism of step leader propagation. The splitting of thunder clouds sat random directions is termed a projectile. This algorithm considers the projectile motion to form a binary tree structure of the step ladder. In the algorithm, these projectiles represent the size of the population. The velocity of the projectile is governed by Equation (7):

$$V_P = \left[1 - \left(\frac{1}{\sqrt{1 - \left(\frac{v_0}{C}\right)^2 - \frac{SF_i}{(mc^2)}}}\right)^{-2}\right]^{\frac{-1}{2}} \tag{7}$$

where s indicates the length of the path traveled, F_i is the constant ionization rate, m represents the projectile's mass, c is the speed of the light in vacuum, and v_0 is the projectile's initial velocity.

The probability of the projectile ionizing a large space is minimal, or the exploration space is less if the mass is low and the travel path is long. Thus, in the algorithm, the Exploration and the exploitation are controlled utilizing the energy intensity relative to various step leaders. Focking is the vital property of the step leading to improving the

solution, and an extra channel is created during this process which increases the population size also. Three types of projectile mark the motion of the step leader. These are the transition projectile, the first step leader population, and the space projectile, which aims to achieve the best position. In contrast, the best position within all populations is considered by the third projectile, which is known as a lead projectile.

The transition projectile is evicted in a random direction. Thus, the standard uniform probability distribution is used for modeling the transition projectile, which is represented in Equation (8):

$$f\left(X^T\right) = \begin{cases} \frac{1}{b} - a & for\ a \leq X^T \leq b \\ 0 & for\ X^T < a \ \ or \ \ X^T > b \end{cases} \tag{8}$$

where X^{T} is the initial tip energy of the step leader i or a random number that generates the solution, a and b are the lower and upper boundaries, respectively. For a population of N step leader, N random projectiles are needed to obtain the solution.

In the next place, after obtaining N step leader tips, the energetic projectile ionizes the surrounding older leader. The exponential distribution of the probability density function is given in Equation (9):

$$f\left(X^S\right) = \begin{cases} \frac{1}{\mu} e^{-X^S/\mu} & for\ X^S \geq 0 \\ 0 & for\ X^S \leq 0 \end{cases} \tag{9}$$

where μ represents the shaping parameter that decides the position or direction of the space projectile in the subsequent step. The position of the projectile is followed by Equation (10):

$$P_{inew}^S = P_i^S \pm \exp rand(\mu_i) \tag{10}$$

where μ_i is the distance from the lead projectile to the space projectile within the algorithm for a considered space projectile, and exp *rand* represents a random number.

For the lead projectile, if the step leader energy is lesser than the projectile energy, then the new position of the space projectile makes sure to expand the channel for step leader propagation. The normal probability distribution function with scalar parameter σ for the lead projectile is shown in Equation (11):

$$f\left(X^L\right) = \frac{1}{\sigma\sqrt{2\pi}} e^{-\left(X^L-\mu\right)^2/2\sigma^2} \tag{11}$$

The following equation can represent the position of the lead projectile:

$$P_{new}^L = P^L + normrand\ (\mu_L, \sigma_L) \tag{12}$$

If the new position of the lead projectile provides a better solution, then the step leader is given an extension, and the position of the lead projectile is updated. The exponential random behavior of the space projectile represents the Exploration and the lead projectile random search represents the exploitation process. These two processes are performed to figure out the optimum solution. The flowchart of the LSA is demonstrated in Figure 1. The control parameters of the algorithm are the maximum number of iterations, the population size, and control time. In this study, these parameters are considered as 100, 70 and 10, respectively.

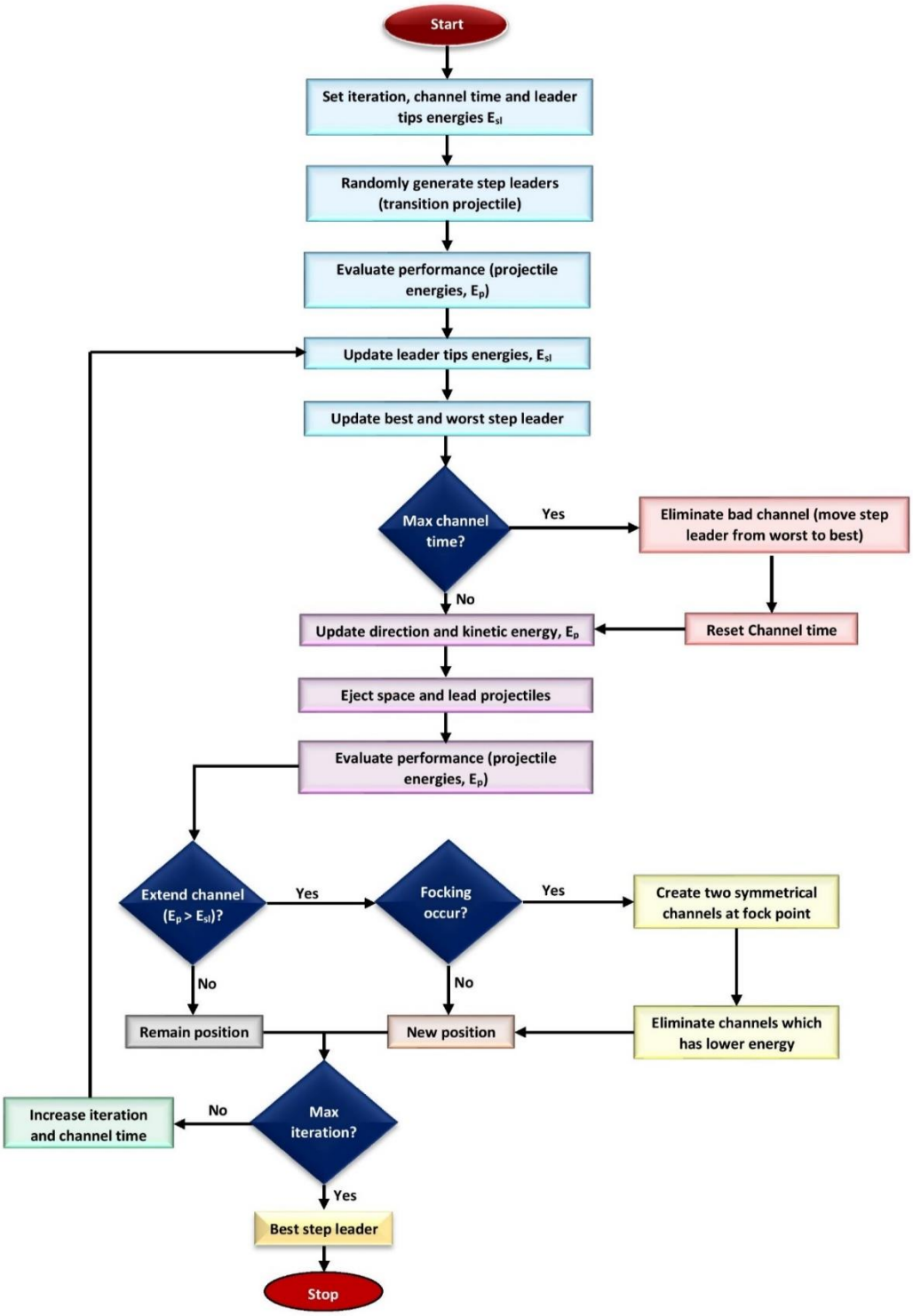

Figure 1. Flowchart of lightning search algorithm (LSA) utilized in this study.

4. The Simulation Results

In this study, the simulation is performed using three commercial fuel cells. The simulation results are depicted under different operating conditions. These results are then compared to the experimental results for more validation. Moreover, these proposed results are compared with the results obtained using other optimization models for more verification. In the first stage, the proposed LSA is applied to minimize the objective function and obtain the PEMFC model's unknown parameters. The second stage illustrates the validation of the proposed model under several operating conditions, such as a variation

in temperature and partial pressure. The lower and upper limit of the design variables is demonstrated in Table 2 [58].

Table 2. Lower and upper limit of design variables.

Parameter	ξ_1	$\xi_2 \times 10^{-3}$	$\xi_3 \times 10^{-5}$	$\xi_4 \times 10^{-5}$	λ	$R_c(m\Omega)$	β
Low	−1.1997	1.00	3.60	−26.00	13.00	0.10	0.0136
High	−0.8532	5.00	9.80	−9.54	23.00	0.80	0.5000

It is worth noting that the optimal parameters of the LSA involve 100 iterations, 70 population agents, and 10 control times. These parameters are fine-tuned by the trial and error method, which is the most commonly used to design the parameters of meta-heuristics algorithms. It depends on the designer's experience to achieve the best performance. To test the robustness of the LSA, 50 independent runs are simultaneously carried out, and all the statistical measurements, such as standard deviation and variance, are very close to zero value. The three commercial PEMFCs are described in detail as follows:

4.1. Ballard Mark V 5 kW

The concerned data and operating conditions are collected from different literature. The stack has 35 cells connected in series with 70-A maximum thermal current. To search the best seven unknown parameter values, the LSA is applied, and after several runs, the best-suited parameters are found and mentioned in Table 3. The convergence characteristic of the fitness function for the PEMFC stack is illustrated in Figure 2. As seen in Figure 2, the convergence curve steadily reduces and reaches a steady value with 100 iterations. The value of the best fitness function is found to be 0.814, as mentioned in Table 3. It is worth noting that the proposed LSA achieves a lower SSE than that obtained using other optimization algorithms, such as the neural network algorithm and the grasshopper optimization algorithm [58]. The polarization characteristics of the proposed LSA-PEMFC model, such as I/V and I/P curves, are plotted in Figure 3a,b, where these curves are compared with their measured data. It can be noted that these simulation responses are very close to the experimental responses meaning that the proposed PEMFC model is accurate. Figure 3c shows the current-voltage characteristics under the oxygen and hydrogen pressure variation. It can be realized that the results lie in an acceptable range.

Table 3. Optimal design variables of the Ballard PEMFC model.

Parameter	LSA	NNA [58]	GOA [58]
ξ_1	−1.0624	−0.97997	−0.8532
$\xi_2 \times 10^{-3}$	3.597	3.6946	3.4173
$\xi_3 \times 10^{-5}$	6.6538	9.0871	9.8000
$\xi_4 \times 10^{-5}$	−16.4925	−16.2820	−15.9555
λ	23.00	23.0000	22.8458
$R_c(\mathrm{m}\Omega)$	0.103	0.1000	0.1000
β	0.0188	0.0136	0.0136
SSE	0.8140	0.85361	0.8710

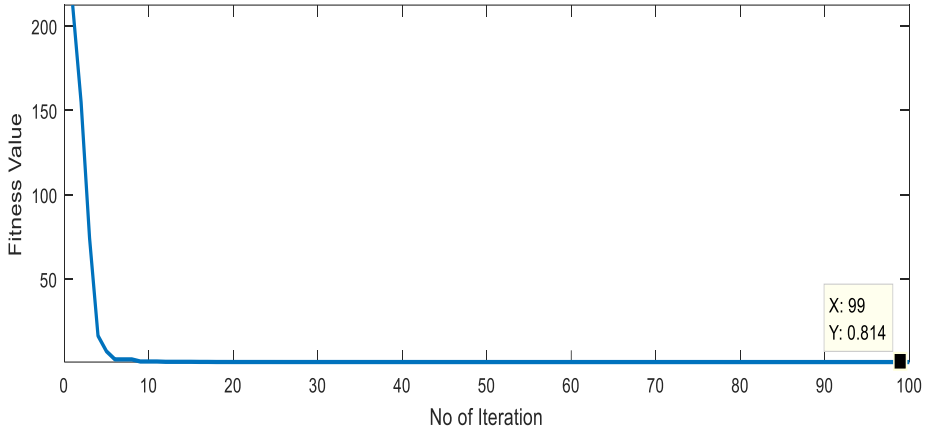

Figure 2. Convergence curve for case-1.

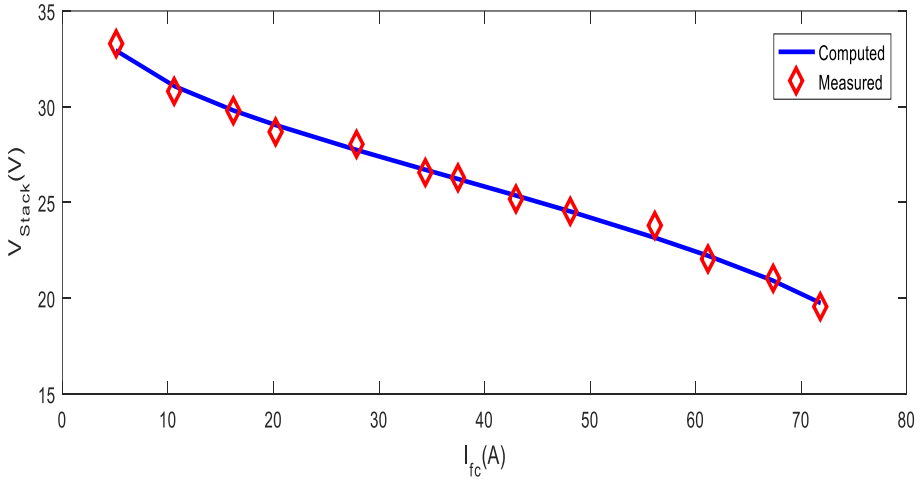

(**a**)

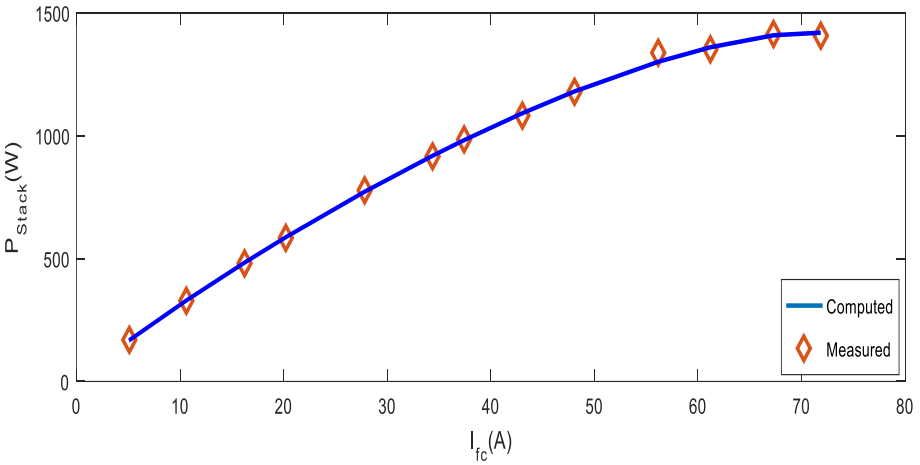

(**b**)

Figure 3. *Cont.*

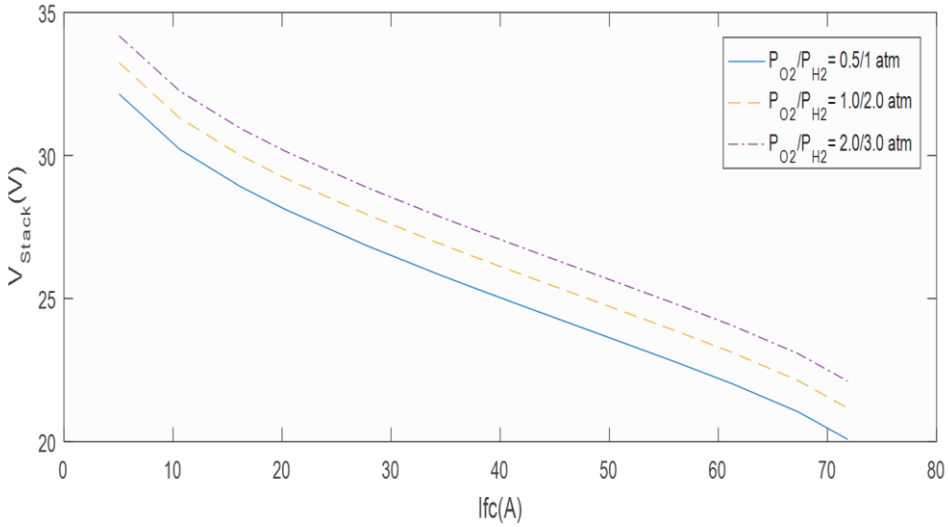

(**c**)

Figure 3. Performance characteristics curves (**a**) I/V curve (**b**) I/P curve (**c**) I/V curve with variation in pressure.

4.2. 500 W BCS PEMFC

In this case study, a 32 cell connected BCS 500 W PEMFC is analyzed. The feature of the stack is found in other literature. The rated current of the stack is 30 A. To search the best seven unknown parameter values, the LSA is applied, and after several runs, the best-suited parameters are found and mentioned in Table 4. The convergence characteristic of the fitness function for the PEMFC stack is illustrated in Figure 4. As seen in Figure 4, the convergence curve steadily reduces and reaches a steady value with 100 iterations. The value of the best fitness function is found to be 0.01169, as mentioned in Table 4. It is worth noting that the proposed LSA achieves a lower SSE than that obtained using the neural network algorithm and salp swarm optimization algorithm [58]. The polarization characteristics of the proposed LSA-PEMFC model, such as I/V and I/P curves, are plotted in Figure 5a,b, where these curves are compared with their measured data. It can be noted that these simulation responses are very close to the experimental responses meaning that the proposed PEMFC model is accurate. Figure 5c shows the current-voltage characteristics under variations of fuel cell temperature. The partial pressure is assumed constant. It can be realized that the results lie in an acceptable range.

Table 4. Optimal design variables of the BCS PEMFC model.

Parameter	LSA	NNA [58]	SSO [58]
ξ_1	−1.0134	−1.0596	−0.8532
$\xi_2 \times 10^{-3}$	2.9662	3.7435	4.8115
$\xi_3 \times 10^{-5}$	5.5693	9.6902	9.4334
$\xi_4 \times 10^{-5}$	−19.2904	−19.3020	−19.205
λ	20.930	20.8772	23.00
$R_c(\mathrm{m}\Omega)$	0.105	0.1000	0.3499
β	0.01609	0.0161	0.01589
SSE	0.011690	0.011698	0.01219

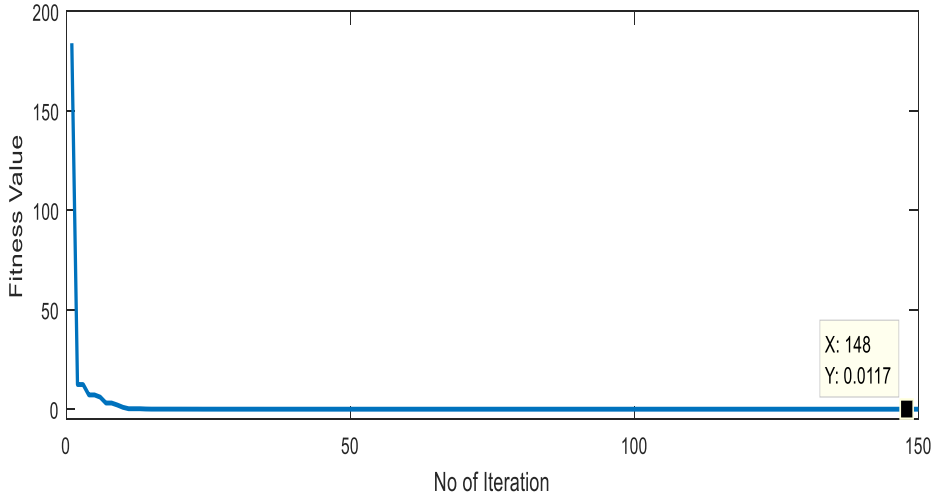

Figure 4. Convergence curve for case-2.

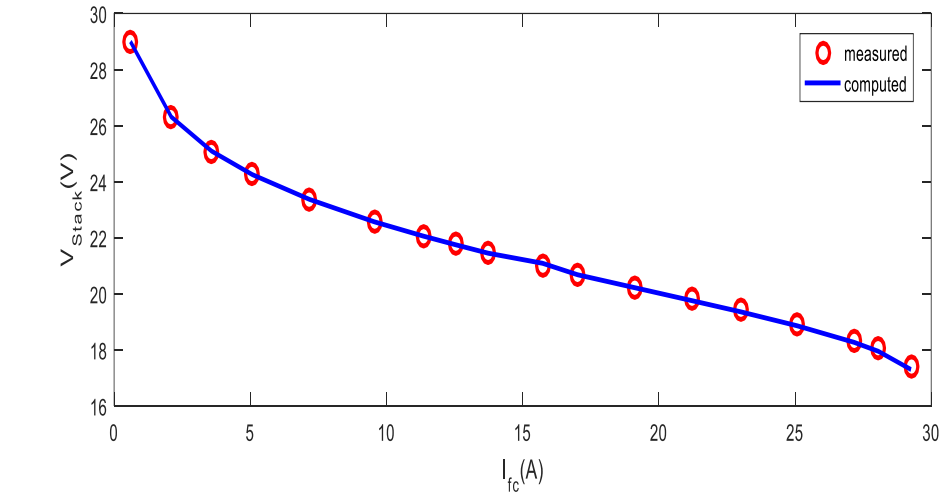

(**a**)

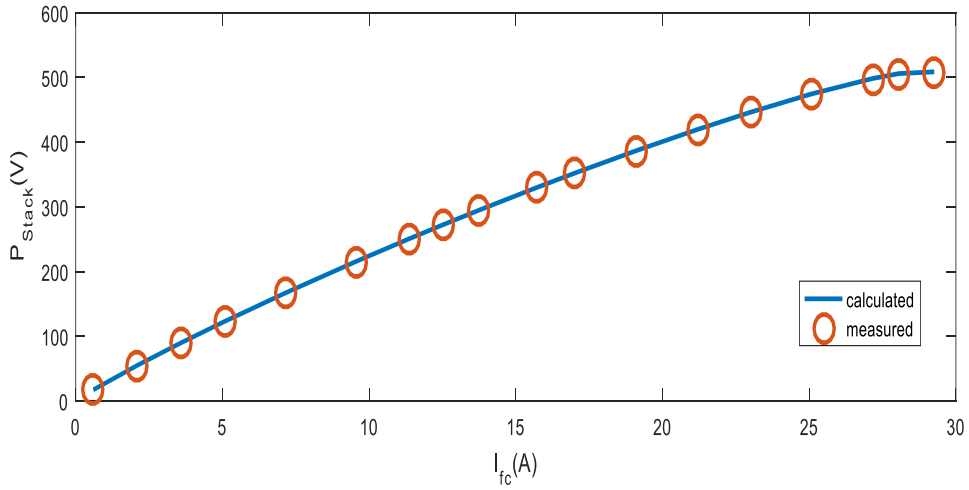

(**b**)

Figure 5. *Cont*.

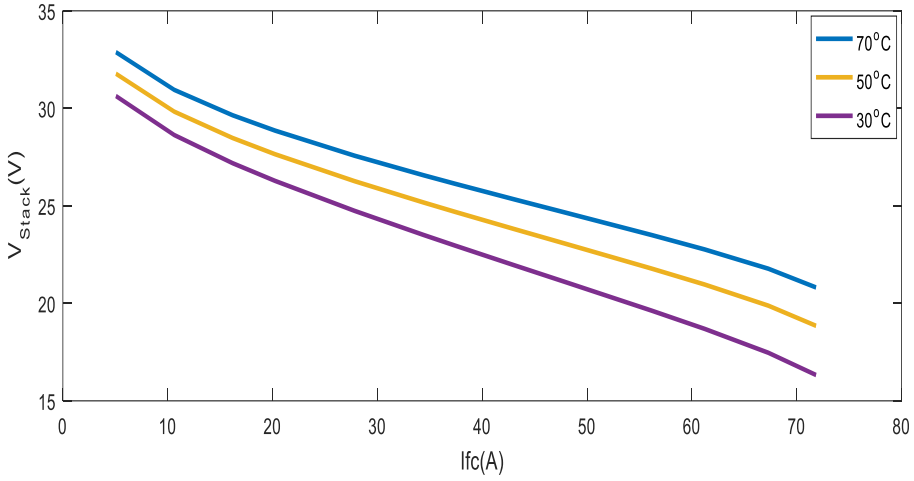

(**c**)

Figure 5. Performance characteristics of the 500 W PEMFC model. (**a**) I/V curve. (**b**) I/P curve. (**c**) I/V curve with temperature variation.

4.3. Nedstack PEMFC

In this case study, 65 series linked cells Nedstack PS6 PEMFC are considered for analysis. The main characteristics of the stack are taken from different literature and compared with different algorithms. The rated current and power of the stack is 225 A and 6 kW, respectively. The LSA is applied to the objective function, and the optimal parameters are listed in Table 5. The convergence characteristic of the fitness function for the PEMFC stack is illustrated in Figure 6. The convergence curve steadily reduces and reaches a steady value with 100 iterations. The value of the best fitness function is found to be 1.996, as mentioned in Table 5. It is worth noting that the proposed LSA achieves a lower SSE than that obtained using other optimization algorithms, such as the neural network algorithm and the salp swarm optimization algorithm [58]. The polarization characteristics of the proposed LSA-PEMFC model, such as I/V and I/P curves, are plotted in Figure 7a,b, where these curves are compared with their measured data. It can be noted that these simulation responses are very close to the experimental responses meaning that the proposed PEMFC model is accurate. Figure 7c,d show the current–voltage characteristics under variable fuel cell temperature and pressure, respectively. It can be realized that the results lie in an acceptable range. As observed from this figure, with an increase in temperature and pressure, the terminal voltage and power increase.

Table 5. Optimal design variables of the Nedstack PEMFC model.

Parameter	LSA	NNA [58]	SSO [58]
ξ_1	−1.0548	−0.8535	−0.9719
$\xi_2 \times 10^{-3}$	3.1687	2.4316	3.3487
$\xi_3 \times 10^{-5}$	4.7606	3.7545	7.9111
$\xi_4 \times 10^{-5}$	−21.211	−9.540	−9.5435
λ	13.015	13.0802	13.00
$R_c(\mathrm{m\Omega})$	0.10	0.10	0.100
β	0.0136	0.0136	0.0534
SSE	1.996	2.14487	2.18067

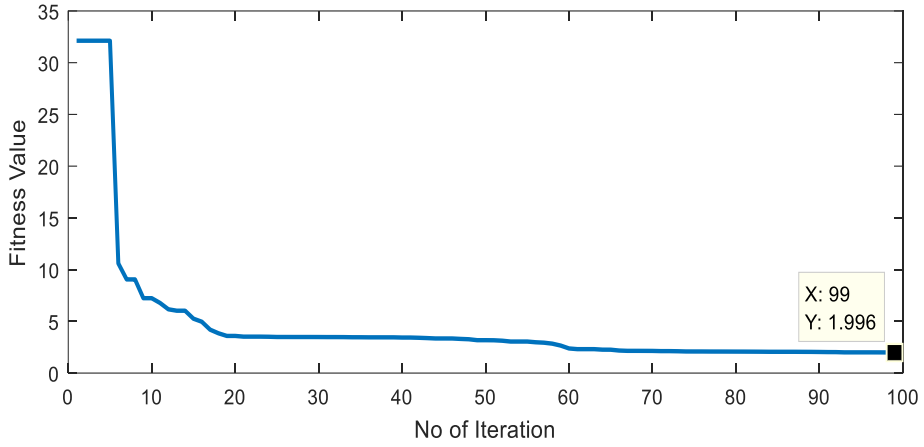

Figure 6. Convergence curve for case-3.

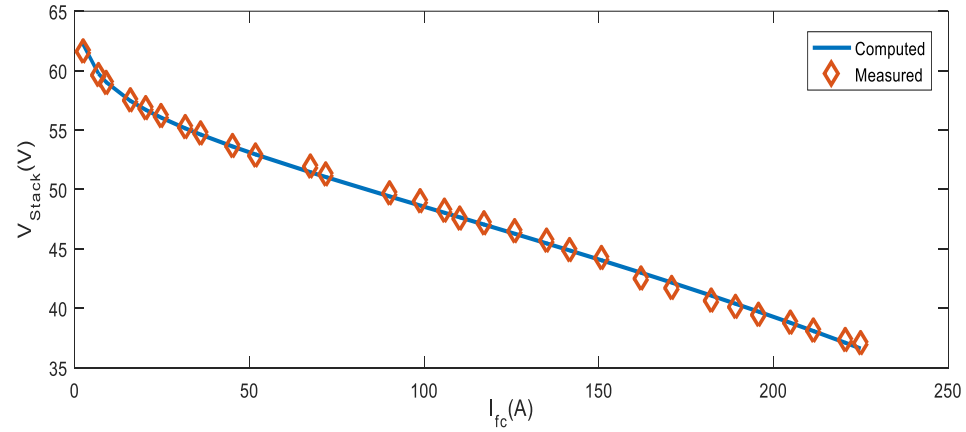

(**a**)

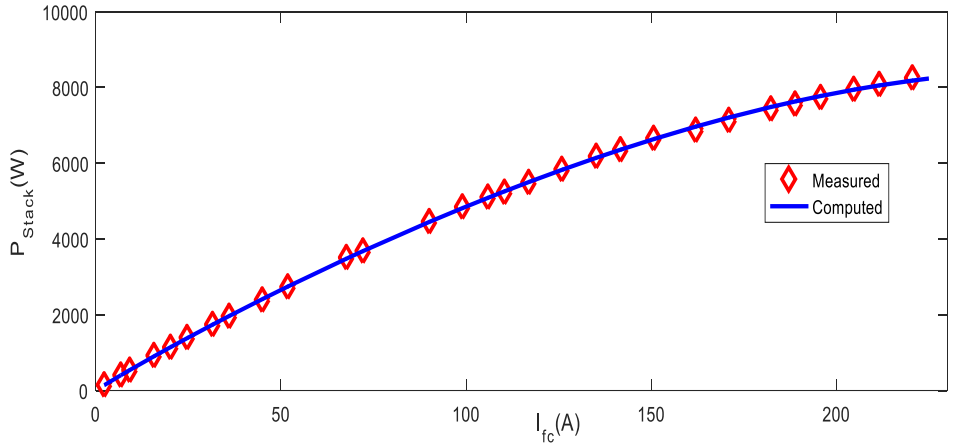

(**b**)

Figure 7. *Cont.*

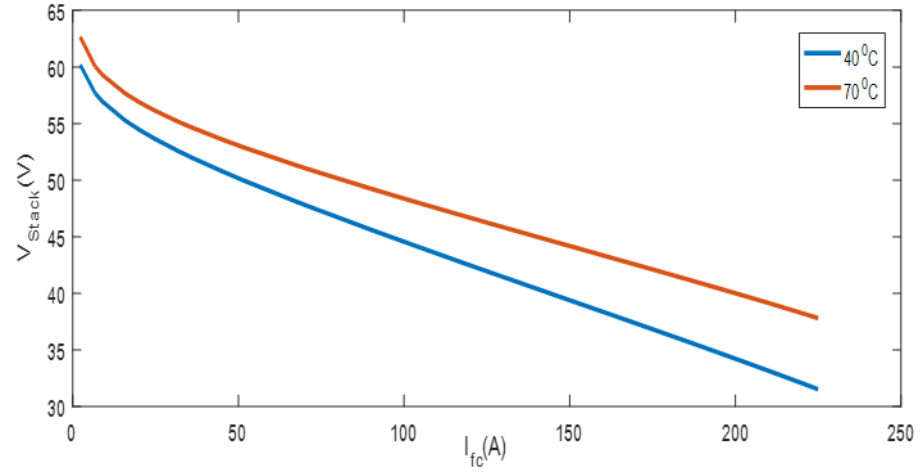

(**c**)

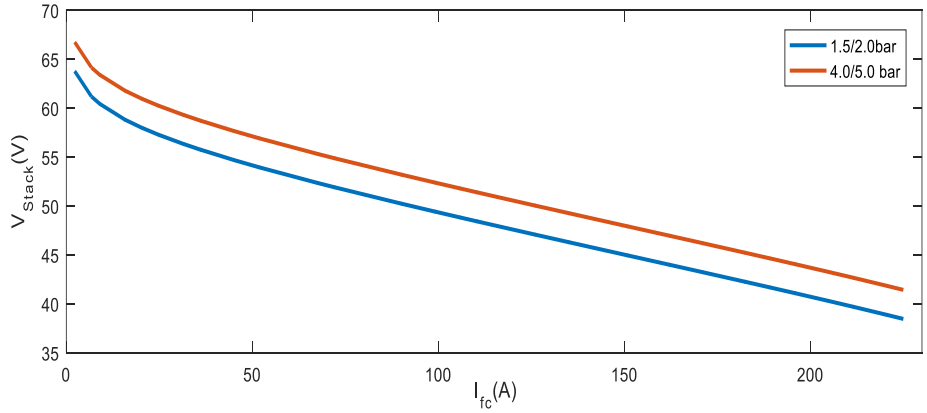

(**d**)

Figure 7. Performance characteristics of NedstackP6S. (**a**) I/V curve. (**b**) I/P curve. (**c**) I/V curve with temperature variation. (**d**) I/V curve with variation in pressure.

5. Conclusions

This study has introduced an attempt to obtain a precise PEMFC model using the LSA. This model highly affects the dynamic and transient analyses of the fuel cell in several simulation studies. Therefore, it is vital to achieving an accurate model of the PEMFC. The LSA is successfully applied to the SSE objective function to yield the design variables of the PEMFC model. The results of this study have shown that the simulation results of the proposed LSA-PEMFC coincide with the experimental results for three commercial PEMFCs. Moreover, a comparison has been made between the proposed model and other optimization algorithms-based models, demonstrating a lower SSE by more than 5% in some cases and high performance of the LSA-PEMFC model. The LSA-PEMFC model results prove its capability under different temperature and pressure conditions. This high performance of the proposed model comes from the proper design of the LSA and its simple and accurate procedures. The LSA shall be applied to solve many other energy and renewable energy problems and smart grid systems.

Author Contributions: Conceptualization, B.M., R.M.E. and H.M.H.; Data curation, B.M., R.M.E. and R.P.; Formal analysis, B.M., R.M.E., H.M.H., E.D., R.A.T. and R.P.; Investigation, B.M., R.M.E., H.M.H., E.D. and R.A.T.; Methodology, B.M., R.M.E., H.M.H. and E.D.; Software, B.M.; Supervision, R.M.E. and H.M.H.; Validation, R.M.E. and H.M.H.; Writing—original draft, B.M., R.M.E., H.M.H. and R.P.; Writing—review & editing, R.M.E., H.M.H., E.D. and R.A.T. All authors contributed equally to publishing this manuscript. All authors have read and agreed to the published version of the manuscript.

Funding: This research received no external funding.

Data Availability Statement: Not applicable.

Conflicts of Interest: The authors declare no conflict of interest.

Nomenclature

A	Membrane area (cm^2)
C_{O_2}	concentration of oxygen in (mol/cm^3)
E_{Nernst}	Reversible voltage of PEMFC (V)
I_{fc}	Operating current of PEMFC (A)
J	Density of actual current (A/cm^2)
J_{max}	Maximum value of $J(A/cm^2)$
l	Membrane thickness (cm)
N_{Cells}	Total number of PEMFC
P_{H_2}	Partial pressure of H_2(atm)
P_{O_2}	Partial pressure of O_2(atm)
P_{H_2O}	Pressure at which H_2O is saturated (atm)
P_a	Inlet pressure of Anode (atm)
P_c	Inlet pressure of Cathode (atm)
R_m	membrane resistance (Ω)
R_c	Connection resistance (Ω)
RH_a	Relative humidity of vapor at Anode
RH_c	Relative humidity of vapor at Cathode
T_{fc}	PEMFC operating temperature (K)
v_{act}	Activation voltage at low current values (V)
v_{con}	Over-potential voltage at high loading (V)
v_R	Ohmic resistive drop at linear operating conditions (V)
v_{Stack}	Overall voltage from PEMFC stack (V)

References

1. Madurai Elavarasan, R.; Pugazhendhi, R.; Irfan, M.; Mihet-Popa, L.; Khan, I.A.; Campana, P.E. State-of-the-art sustainable approaches for deeper decarbonization in Europe—An endowment to climate neutral vision. *Renew. Sustain. Energy Rev.* **2022**, *159*, 112204. [CrossRef]
2. Moriarty, P.; Honnery, D. Renewable Energy and Energy Reductions or Solar Geoengineering for Climate Change Mitigation? *Energies* **2022**, *15*, 7315. [CrossRef]
3. Kochanek, E. The Role of Hydrogen in the Visegrad Group Approach to Energy Transition. *Energies* **2022**, *15*, 7235. [CrossRef]
4. Taner, T. Energy and exergy analyze of PEM fuel cell: A case study of modeling and simulations. *Energy* **2018**, *143*, 284–294. [CrossRef]
5. Huang, X.; Zhang, Z.; Jiang, J. Fuel Cell Technology for Distributed Generation: An Overview. In Proceedings of the 2006 IEEE International Symposium on Industrial Electronics, Montreal, QC, Canada, 9–13 July 2006; pp. 1613–1618.
6. Springer, T.E.; Zawodzinski, T.A.; Gottesfeld, S. Polymer Electrolyte Fuel Cell Model. *J. Electrochem. Soc.* **1991**, *138*, 2334–2342. [CrossRef]
7. Papadopoulos, P.N.; Kandyla, M.; Kourtza, P.; Papadopoulos, T.A.; Papagiannis, G.K. Parametric analysis of the steady state and dynamic performance of proton exchange membrane fuel cell models. *Renew. Energy* **2014**, *71*, 23–31. [CrossRef]
8. Arun Kumar, P.; Geetha, M.; Chandran, K.R.; Sanjeevikumar, P. PEM Fuel Cell System Identification and Control. In *Advances in Smart Grid and Renewable Energy*; Springer: Berlin/Heidelberg, Germany, 2018; pp. 449–457.
9. Solsona, M.; Kunusch, C.; Ocampo-Martinez, C. Control-oriented model of a membrane humidifier for fuel cell applications. *Energy Convers. Manag.* **2017**, *137*, 121–129. [CrossRef]
10. Gong, W.; Yan, X.; Hu, C.; Wang, L.; Gao, L. Fast and accurate parameter extraction for different types of fuel cells with decomposition and nature-inspired optimization method. *Energy Convers. Manag.* **2018**, *174*, 913–921. [CrossRef]

11. Li, J.; Gao, X.; Cui, Y.; Hu, J.; Xu, G.; Zhang, Z. Accurate, efficient and reliable parameter extraction of PEM fuel cells using shuffled multi-simplexes search algorithm. *Energy Convers. Manag.* **2020**, *206*, 112501. [CrossRef]
12. Hu, Z.; Xu, L.; Li, J.; Gan, Q.; Xu, X.; Ouyang, M.; Song, Z.; Kim, J. A multipoint voltage-monitoring method for fuel cell inconsistency analysis. *Energy Convers. Manag.* **2018**, *177*, 572–581. [CrossRef]
13. Wang, B.; Xie, B.; Xuan, J.; Jiao, K. AI-based optimization of PEM fuel cell catalyst layers for maximum power density via data-driven surrogate modeling. *Energy Convers. Manag.* **2020**, *205*, 112460. [CrossRef]
14. Xiong, G.; Shi, D.; Zhang, J.; Zhang, Y. A binary coded brain storm optimization for fault section diagnosis of power systems. *Electr. Power Syst. Res.* **2018**, *163*, 441–451. [CrossRef]
15. Yang, B.; Wang, J.; Zhang, M.; Shu, H.; Yu, T.; Zhang, X.; Yao, W.; Sun, L. A state-of-the-art survey of solid oxide fuel cell parameter identification: Modelling, methodology, and perspectives. *Energy Convers. Manag.* **2020**, *213*, 112856. [CrossRef]
16. Guo, C.; Lu, J.; Tian, Z.; Guo, W.; Darvishan, A. Optimization of critical parameters of PEM fuel cell using TLBO-DE based on Elman neural network. *Energy Convers. Manag.* **2019**, *183*, 149–158. [CrossRef]
17. Yu, D.; Wang, Y.; Liu, H.; Jermsittiparsert, K.; Razmjooy, N. System identification of PEM fuel cells using an improved Elman neural network and a new hybrid optimization algorithm. *Energy Rep.* **2019**, *5*, 1365–1374. [CrossRef]
18. Turgut, O.E.; Coban, M.T. Optimal proton exchange membrane fuel cell modelling based on hybrid Teaching Learning Based Optimization—Differential Evolution algorithm. *Ain Shams Eng. J.* **2016**, *7*, 347–360. [CrossRef]
19. Cao, Y.; Kou, X.; Wu, Y.; Jermsittiparsert, K.; Yildizbasi, A. PEM fuel cells model parameter identification based on a new improved fluid search optimization algorithm. *Energy Rep.* **2020**, *6*, 813–823. [CrossRef]
20. Cao, Y.; Li, Y.; Zhang, G.; Jermsittiparsert, K.; Razmjooy, N. Experimental modeling of PEM fuel cells using a new improved seagull optimization algorithm. *Energy Rep.* **2019**, *5*, 1616–1625. [CrossRef]
21. Guo, Y.; Dai, X.; Jermsittiparsert, K.; Razmjooy, N. An optimal configuration for a battery and PEM fuel cell-based hybrid energy system using developed Krill herd optimization algorithm for locomotive application. *Energy Rep.* **2020**, *6*, 885–894. [CrossRef]
22. Tian, M.-W.; Yan, S.-R.; Han, S.-Z.; Nojavan, S.; Jermsittiparsert, K.; Razmjooy, N. New optimal design for a hybrid solar chimney, solid oxide electrolysis and fuel cell based on improved deer hunting optimization algorithm. *J. Clean. Prod.* **2020**, *249*, 119414. [CrossRef]
23. Bizon, N. Energy optimization of fuel cell system by using global extremum seeking algorithm. *Appl. Energy* **2017**, *206*, 458–474. [CrossRef]
24. Chen, Y.; Wang, N. Cuckoo search algorithm with explosion operator for modeling proton exchange membrane fuel cells. *Int. J. Hydrogen Energy* **2019**, *44*, 3075–3087. [CrossRef]
25. Piela, P.; Mitzel, J.; Gülzow, E.; Hunger, J.; Kabza, A.; Jörissen, L.; Valle, F.; Pilenga, A.; Malkow, T.; Tsotridis, G. Performance optimization of polymer electrolyte membrane fuel cells using the Nelder-Mead algorithm. *Int. J. Hydrogen Energy* **2017**, *42*, 20187–20200. [CrossRef]
26. Nejad, H.C.; Farshad, M.; Gholamalizadeh, E.; Askarian, B.; Akbarimajd, A. A novel intelligent-based method to control the output voltage of Proton Exchange Membrane Fuel Cell. *Energy Convers. Manag.* **2019**, *185*, 455–464. [CrossRef]
27. Chakraborty, U.K. Static and dynamic modeling of solid oxide fuel cell using genetic programming. *Energy* **2009**, *34*, 740–751. [CrossRef]
28. Yang, J.; Li, X.; Jiang, J.H.; Jian, L.; Zhao, L.; Jiang, J.G.; Wu, X.G.; Xu, L.H. Parameter optimization for tubular solid oxide fuel cell stack based on the dynamic model and an improved genetic algorithm. *Int. J. Hydrogen Energy* **2011**, *36*, 6160–6174. [CrossRef]
29. Chakraborty, U.K.; Abbott, T.E.; Das, S.K. PEM fuel cell modeling using differential evolution. *Energy* **2012**, *40*, 387–399. [CrossRef]
30. Gong, W.; Yan, X.; Liu, X.; Cai, Z. Parameter extraction of different fuel cell models with transferred adaptive differential evolution. *Energy* **2015**, *86*, 139–151. [CrossRef]
31. del Valle, Y.; Venayagamoorthy, G.K.; Mohagheghi, S.; Hernandez, J.-C.; Harley, R.G. Particle Swarm Optimization: Basic Concepts, Variants and Applications in Power Systems. *IEEE Trans. Evol. Comput.* **2008**, *12*, 171–195. [CrossRef]
32. Jiang, B.; Wang, N.; Wang, L. Parameter identification for solid oxide fuel cells using cooperative barebone particle swarm optimization with hybrid learning. *Int. J. Hydrogen Energy* **2014**, *39*, 532–542. [CrossRef]
33. Sultan, H.M.; Menesy, A.S.; Kamel, S.; Selim, A.; Jurado, F. Parameter identification of proton exchange membrane fuel cells using an improved salp swarm algorithm. *Energy Convers. Manag.* **2020**, *224*, 113341. [CrossRef]
34. Yang, B.; Yu, T.; Zhang, X.; Li, H.; Shu, H.; Sang, Y.; Jiang, L. Dynamic leader based collective intelligence for maximum power point tracking of PV systems affected by partial shading condition. *Energy Convers. Manag.* **2019**, *179*, 286–303. [CrossRef]
35. Zhang, W.; Wang, N.; Yang, S. Hybrid artificial bee colony algorithm for parameter estimation of proton exchange membrane fuel cell. *Int. J. Hydrogen Energy* **2013**, *38*, 5796–5806. [CrossRef]
36. Saremi, S.; Mirjalili, S.; Lewis, A. Grasshopper Optimisation Algorithm: Theory and application. *Adv. Eng. Softw.* **2017**, *105*, 30–47. [CrossRef]
37. Zakeri, A.; Hokmabadi, A. Efficient feature selection method using real-valued grasshopper optimization algorithm. *Expert Syst. Appl.* **2019**, *119*, 61–72. [CrossRef]
38. Wei, Y.; Stanford, R.J. Parameter identification of solid oxide fuel cell by Chaotic Binary Shark Smell Optimization method. *Energy* **2019**, *188*, 115770. [CrossRef]
39. Rao, Y.; Shao, Z.; Ahangarnejad, A.H.; Gholamalizadeh, E.; Sobhani, B. Shark Smell Optimizer applied to identify the optimal parameters of the proton exchange membrane fuel cell model. *Energy Convers. Manag.* **2019**, *182*, 1–8. [CrossRef]

40. Gandomi, A.H. Interior search algorithm (ISA): A novel approach for global optimization. *ISA Trans.* **2014**, *53*, 1168–1183. [CrossRef]
41. Kler, D.; Rana, K.P.S.; Kumar, V. Parameter extraction of fuel cells using hybrid interior search algorithm. *Int. J. Energy Res.* **2019**, *43*, 2854–2880. [CrossRef]
42. Mirjalili, S.; Gandomi, A.H.; Mirjalili, S.Z.; Saremi, S.; Faris, H.; Mirjalili, S.M. Salp Swarm Algorithm: A bio-inspired optimizer for engineering design problems. *Adv. Eng. Softw.* **2017**, *114*, 163–191. [CrossRef]
43. Mirjalili, S.; Mirjalili, S.M.; Lewis, A. Grey Wolf Optimizer. *Adv. Eng. Softw.* **2014**, *69*, 46–61. [CrossRef]
44. Fathy, A.; Rezk, H. Multi-verse optimizer for identifying the optimal parameters of PEMFC model. *Energy* **2018**, *143*, 634–644. [CrossRef]
45. Cheng, R.; Jin, Y. A Competitive Swarm Optimizer for Large Scale Optimization. *IEEE Trans. Cybern.* **2015**, *45*, 191–204. [CrossRef] [PubMed]
46. Xiong, G.; Zhang, J.; Shi, D.; Yuan, X. A simplified competitive swarm optimizer for parameter identification of solid oxide fuel cells. *Energy Convers. Manag.* **2020**, *203*, 112204. [CrossRef]
47. Mirjalili, S.; Lewis, A. The Whale Optimization Algorithm. *Adv. Eng. Softw.* **2016**, *95*, 51–67. [CrossRef]
48. El-Fergany, A.A.; Hasanien, H.M.; Agwa, A.M. Semi-empirical PEM fuel cells model using whale optimization algorithm. *Energy Convers. Manag.* **2019**, *201*, 112197. [CrossRef]
49. Simon, D. Biogeography-Based Optimization. *IEEE Trans. Evol. Comput.* **2008**, *12*, 702–713. [CrossRef]
50. Niu, Q.; Zhang, L.; Li, K. A biogeography-based optimization algorithm with mutation strategies for model parameter estimation of solar and fuel cells. *Energy Convers. Manag.* **2014**, *86*, 1173–1185. [CrossRef]
51. Samareh Moosavi, S.H.; Khatibi Bardsiri, V. Satin bowerbird optimizer: A new optimization algorithm to optimize ANFIS for software development effort estimation. *Eng. Appl. Artif. Intell.* **2017**, *60*, 1–15. [CrossRef]
52. El-Hay, E.A.; El-Hameed, M.A.; El-Fergany, A.A. Steady-state and dynamic models of solid oxide fuel cells based on Satin Bowerbird Optimizer. *Int. J. Hydrogen Energy* **2018**, *43*, 14751–14761. [CrossRef]
53. Askarzadeh, A.; dos Santos Coelho, L. A backtracking search algorithm combined with Burger's chaotic map for parameter estimation of PEMFC electrochemical model. *Int. J. Hydrogen Energy* **2014**, *39*, 11165–11174. [CrossRef]
54. Rao, R.V.; Savsani, V.J.; Vakharia, D.P. Teaching–learning-based optimization: A novel method for constrained mechanical design optimization problems. *Comput. Des.* **2011**, *43*, 303–315. [CrossRef]
55. Xiong, G.; Zhang, J.; Shi, D.; He, Y. Parameter identification of solid oxide fuel cells with ranking teaching-learning based algorithm. *Energy Convers. Manag.* **2018**, *174*, 126–137. [CrossRef]
56. Shareef, H.; Ibrahim, A.A.; Mutlag, A.H. Lightning search algorithm. *Appl. Soft Comput.* **2015**, *36*, 315–333. [CrossRef]
57. Panigrahy, D.; Samal, P. Modified lightning search algorithm for optimization. *Eng. Appl. Artif. Intell.* **2021**, *105*, 104419. [CrossRef]
58. Elsisi, M.; Abdelfattah, H. New design of variable structure control based on lightning search algorithm for nuclear reactor power system considering load-following operation. *Nucl. Eng. Technol.* **2020**, *52*, 544–551. [CrossRef]
59. Ali, J.A.; Hannan, M.A.; Mohamed, A.; Pin Jern, K.; Abdolrasol, M.G. Implementation of DSP-based optimal fuzzy logic speed controller for IM drive using quantum lightning search algorithm. *Measurement* **2020**, *153*, 107372. [CrossRef]
60. Aljanad, A.; Mohamed, A.; Shareef, H.; Khatib, T. A novel method for optimal placement of vehicle-to-grid charging stations in distribution power system using a quantum binary lightning search algorithm. *Sustain. Cities Soc.* **2018**, *38*, 174–183. [CrossRef]
61. Thangaraj, Y.; Kuppan, R. Multi-objective simultaneous placement of DG and DSTATCOM using novel lightning search algorithm. *J. Appl. Res. Technol.* **2017**, *15*, 477–491. [CrossRef]
62. Moreno, S.R.; Pierezan, J.; dos Santos Coelho, L.; Mariani, V.C. Multi-objective lightning search algorithm applied to wind farm layout optimization. *Energy* **2021**, *216*, 119214. [CrossRef]
63. Fawzi, M.; El-Fergany, A.A.; Hasanien, H.M. Effective methodology based on neural network optimizer for extracting model parameters of PEM fuel cells. *Int. J. Energy Res.* **2019**, *43*, 8136–8147. [CrossRef]
64. Selem, S.I.; Hasanien, H.M.; El-Fergany, A.A. Parameters extraction of PEMFC's model using manta rays foraging optimizer. *Int. J. Energy Res.* **2020**, *44*, 4629–4640. [CrossRef]